

This is a provisional PDF only. Copyedited and fully formatted version will be made available soon.



CARDIOLOGY
JOURNAL

ISSN: 1897-5593
e-ISSN: 1898-018X

Stabilization of unstable reentrant atrial tachycardias via fractionated continuous electrical activity ablation (CHAOS study)

Authors: Eduardo Franco, Cristina Lozano Granero, Roberto Matía, Antonio Hernández-Madrid, Inmaculada Sánchez Pérez, José Luis Zamorano, Javier Moreno

DOI: 10.5603/CJ.a2022.0036

Article type: Original Article

Submitted: 2021-08-05

Accepted: 2021-11-19

Published online: 2022-05-13

This article has been peer reviewed and published immediately upon acceptance. It is an open access article, which means that it can be downloaded, printed, and distributed freely, provided the work is properly cited. Articles in "Cardiology Journal" are listed in PubMed.

Stabilization of unstable reentrant atrial tachycardias via fractionated continuous electrical activity ablation (CHAOS study)

Eduardo Franco et al., Stabilization of unstable reentrant atrial tachycardias

Eduardo Franco¹, Cristina Lozano Granero¹, Roberto Matía¹, Antonio Hernández-Madrid¹, Inmaculada Sánchez², José Luis Zamorano¹, Javier Moreno¹

¹Arrhythmia Unit, Cardiology Department, University Hospital Ramón y Cajal, Madrid, Spain

²Pediatric Cardiology Department, University Hospital Ramón y Cajal, Madrid, Spain

Address for correspondence: Eduardo Franco, MD, PhD, Arrhythmia Unit, Cardiology Department, University Hospital Ramón y Cajal, Carretera de Colmenar Viejo, Km 9.100, ZIP: 28034, Madrid, Spain, tel: +34 913 36 9006, fax: +34 913 36 8515, e-mail: efranco@academiamir.com

ABSTRACT

Background: Unstable reentrant atrial tachycardias (ATs) (i.e., those with frequent circuit modification or conversion to atrial fibrillation) are challenging to ablate. We tested a strategy to achieve arrhythmia stabilization into mappable stable ATs based on the detection and ablation of rotors.

Methods: All consecutive patients from May 2017 to December 2019 were included. Mapping was performed using conventional high-density mapping catheters (IntellaMap ORION, PentaRay NAV, or Advisor HD Grid). Rotors were subjectively identified as fractionated continuous (or quasi-continuous) electrograms on 1–2 adjacent bipoles, without dedicated software. In patients without detectable rotors, sites with spatiotemporal dispersion (i.e., all the cycle length comprised within the mapping catheter) plus non-continuous fractionation on single bipoles were targeted. Ablation success was defined as conversion to a stable AT or sinus rhythm.

Results: Ninety-seven patients with reentrant ATs were ablated. Of these, 18 (18.6%) presented unstable circuits. Thirteen (72%) patients had detectable rotors (median 2 [1–3])

rotors per patient); focal ablation was successful in 12 (92%). In the other 5 patients, 17 sites with spatiotemporal dispersion were identified and targeted. Globally, and excluding one patient with spontaneous AT stabilization, ablation success was achieved in 16/17 patients (94.1%). One-year freedom from atrial arrhythmias was similar between patients with unstable and stable ATs (66.7% vs. 65.8%, $p = 0.946$).

Conclusions: Most unstable reentrant ATs show detectable rotors, identified as sites with single-bipole fractionated quasi-continuous signals, or spatiotemporal dispersion plus non-continuous fractionation. Ablation of these sites is highly effective to stabilize the AT or convert it into sinus rhythm.

Key words: atypical atrial flutter, atrial tachycardia, ablation, rotor, high-density mapping

INTRODUCTION

Reentrant atrial tachycardias (ATs), excluding cavotricuspid isthmus (CTI)-dependent atrial flutter, can be challenging to map, especially in unstable circuits (i.e., those with frequent circuit modification or conversion to atrial fibrillation [AF]). These cases, which account for up to 15–20% [1, 2], are considered non-mappable and ablation is frequently not attempted. Electrical cardioversion and re-induction of the clinical AT can be tried, but arrhythmia induction and stabilization is often difficult to achieve. Class Ic antiarrhythmic agents can be used for this purpose [3], but modification of atrial conduction properties can lead to non-clinical ATs. Another strategy is to perform substrate mapping and ablation in sinus rhythm [4].

Patients with unstable circuits have been excluded from most reentrant AT ablation series, which have focused on mappable circuits [1, 2, 5–9]. These patients are frequently considered untreatable with ablation, and this may lead to cessation of rhythm control and acceptance that the atrial arrhythmia is permanent. In recent years, ablation strategies that try to terminate AF via identification and ablation of AF drivers (rotational or focal) have emerged [10]. Another approach is to ablate areas with electrical spatiotemporal dispersion (STD) as a surrogate of local rotational activation [11]. Given the known relationship between AF and reentrant ATs [12], we hypothesized that these strategies, specifically ablation of sites with rotational activation (i.e., rotors), might as well be used to stabilize or terminate unstable reentrant ATs.

The conversion of hardly mappable atrial tachycardias via rotor ablation into sinus rhythm (CHAOS) study was a prospective single-center study, designed to test an ablation strategy in patients with unstable reentrant ATs based on the ablation of rotors, which were subjectively identified with conventional high-density mapping catheters as sites with fractionated quasi-continuous electrograms (EGMs) on 1–2 adjacent bipoles.

METHODS

The single-center CHAOS study prospectively included all patients scheduled for reentrant AT ablation from May 2017 to December 2019, excluding patients diagnosed with CTI-dependent atrial flutter, in which the tachycardia circuit was deemed non-mappable due to continuous circuit modification or conversion to AF. All patients had pre-procedural documentation of reentrant AT on the surface electrocardiogram (ECG) based on the following: 1) the presence of continuous atrial activity on the surface ECG, or: 2) in patients with focal AT pattern, the arrhythmia behavior (stable cycle length without modification at onset or end) and patient characteristics (diseased atria) [13]. Patients could present to the ablation procedure in sinus rhythm, AT or AF.

Procedures

After achieving echography-guided femoral vein access, a 24-pole diagnostic catheter (Woven Orbiter, Boston Scientific Inc.) was placed around the tricuspid annulus with its distal part in the coronary sinus. If the initial rhythm was AT, entrainment from both right and left atria (via coronary sinus) was used to define AT origin. If the patient was in sinus rhythm, atrial programmed stimulation with ramps was first used to induce AT.

Patients were included if AF was induced or conversion from AT to AF (or continuous AT circuit changes, considered equivalent to AF) happened during the procedure and no spontaneous re-conversion to a stable AT occurred during the following 15 min. Also, patients with AF as the initial rhythm were included.

Mapping protocol and rotor identification

Mapping was performed using conventional high-density electroanatomical mapping catheters (IntellaMap ORION, Boston Scientific Inc.; PentaRay NAV, Biosense Webster Inc.;

or Advisor HD Grid, Abbott Medical Inc.) and their respective mapping system (Rhythmia, Carto3, or Ensite Precision).

Rotors were subjectively identified as fractionated continuous (or quasi-continuous) bipolar EGMs on 1–2 adjacent bipoles of the mapping catheter, using a digital recorder (Bard LabSystem Pro) at 200 mm/s speed (Fig. 1A). When such EGMs were identified, the mapping catheter was kept still for 10 s to confirm temporal stability of the rotor, which was then annotated with a manual marker deployed on an electroanatomical bipolar voltage map.

If rotors were absent in both atria, or rotor ablation was unsuccessful to stabilize or terminate AF, sites with STD (i.e., all the AF cycle length comprised within the different bipoles of the mapping catheters) plus non-continuous fragmentation on single bipoles, arbitrarily defined as continuous bipolar EGMs with > 4 deflections and total duration > 70 ms, were manually annotated and targeted for ablation (Fig. 1B). At least 10 s of temporal stability was also required for these sites.

Ablation protocol

Radiofrequency ablation was performed using open-tip irrigated catheters (IntellaNav MIFI, Boston Scientific Inc.; Thermocool SmartTouch, Biosense Webster Inc.; TactiCath, Abbott Medical Inc.; or TactiCath, Sensor Enabled, Abbott Medical Inc.). First, focal ablation of the identified rotors was performed with 1–4 adjacent lesions. If rotor ablation was unsuccessful, sites with STD were targeted using the same focal approach.

Rotor ablation success was defined, for each patient, as conversion to sinus rhythm or a stable AT using the aforementioned strategy. If rotors were present within the pulmonary veins antra, circumferential pulmonary vein isolation (PVI) of that vein or pair of veins was performed including the rotor within the line. If rotor ablation was performed < 1 cm from a scar or another radiofrequency application, an ablation line between them was performed. If rotor ablation was not successful, electrical cardioversion and empirical PVI plus CTI ablation was performed.

All stable ATs were mapped using local activation time mapping, propagation mapping and entrainment, and subsequently ablated. In the case of conversion to another AT, the new AT was mapped and ablated. If the patient had undergone previous ablation procedures, bidirectional block of the previously performed lines (including circumferential PVI in patients with prior AF ablation) was checked, and ablation was performed if gaps were

present. Pulmonary vein isolation was not performed in all patients, but it was routinely completed in those with previously documented AF.

Finally, programmed atrial stimulation was used to test arrhythmia inducibility; if other sustained ATs were induced, they were mapped and ablated. Procedural success was defined as the successful ablation of all inducible ATs, without requiring electrical cardioversion, with final sinus rhythm and non-inducibility at the end of the procedure.

Follow-up

Patients were followed up with clinical visits and 24-h Holter monitoring at 3, 6, and 12 months. Any arrhythmia lasting > 30 s, according to patients' symptoms or documented on Holter monitoring, was considered a recurrence. A blanking period of 3 months, in which recurrences were mostly treated with electrical cardioversion, was considered.

Statistical analysis

Categorical variables are described as number (percentage) and were compared with the χ^2 or Fisher's exact test, as appropriate. Continuous variables are described as mean \pm standard deviation for variables with normal distributions or as median (interquartile range) for variables not normally distributed. The Kolmogorov-Smirnov test was used to assess normality in continuous variables. Comparisons among normal continuous variables were made using Student's t tests (normal variables) or Mann-Whitney U tests (for variables not normally distributed). Bilateral p values < 0.05 were considered statistically significant. For survival analysis (recurrence of atrial arrhythmias), the Kaplan-Meier method was used. Statistical analysis was performed using SPSS Statistics Base version 22.0 package (IBM Inc., Armonk, NY).

RESULTS

From May 2017 to December 2019, 97 patients were scheduled for reentrant AT ablation, excluding CTI-dependent atrial flutter. Of these, 18 (18.6%) patients presented non-mappable circuits and were included (Table 1). Seven (39%) patients were > 75 years of age, and 4 (22%) patients were > 80 years of age. Seven (39%) patients had severe left atrium dilation. Mean procedural time was 265 \pm 67 min, and mean fluoroscopy use, expressed as

dose-product area, was $28,499 \pm 10,212$ mGy · cm². Of note, only 5 patients were on rhythm control drugs (flecainide, n = 2; propafenone, n = 1; sotalol, n = 1; and amiodarone, n = 1) before the index procedure.

The included patients (with non-mappable circuits) had less enlarged left atria than those with mappable circuits.

Mapping and rotor ablation

Among the 18 included patients, 14 (77.7%) presented to the ablation procedure in sinus rhythm; in 12 patients, an AT was induced but was considered not mappable due to conversion to AF (n = 10) or continuous circuit modification (n = 2); in the other 2 patients, programmed atrial stimulation directly induced AF. Three (16.7%) patients presented in AT; in 2 of them, conversion to AF during mapping occurred; in the other patient, after successful ablation of the index AT, programmed atrial stimulation induced AF. One (5.6%) patient presented in AF.

Mapping was performed with PentaRay NAV catheter (Carto3) in 5 (28%) patients, with IntellaMap ORION (Rhythmia) in 11 (61%) patients, and with Advisor HD Grid (Ensite Precision) in 2 (11%) patients. There were no significant differences among the mapping catheters in the presence or number of detected rotors or sites with STD and non-continuous fragmentation; also, operators did not perceive subjective differences in mapping performance using the 3 catheters. Contact force-sensing catheters were used for ablation in 6 (33.3%) patients. In 9 (50%) patients, rotor mapping and ablation was performed only in the left atrium; in 1 patient, only in the right atrium; and in the other 8 (44.4%) patients, both atria were mapped. The median number of acquired points with each mapping system is shown in **Supplementary Table 1**. The detailed rotor mapping and ablation approach is shown in Figure 2.

Rotors, defined as sites with fractionated quasi-continuous signals on 1–2 adjacent bipoles of the mapping catheter, were found in 13 (72%) patients (median 2 [1–3] rotors per patient) (Fig. 3A); all detected rotors showed temporal permanence after mapping and were a target of ablation. Focal rotor ablation was effective in 12 (92%) of these patients; in the other patient, after unsuccessful rotor ablation, 2 sites with STD and non-continuous fragmentation were detected and successfully ablated to stabilize AF into reentrant AT. In one patient without detectable rotors, spontaneous stabilization of AF into reentrant AT happened during

mapping, and AT ablation could be successfully performed. In the other 4 patients without rotors, sites with STD and non-continuous fragmentation were detected (2, 3, 4, and 6 sites in each patient) (Fig. 3B); ablation of these sites resulted in arrhythmia stabilization into AT in 3 (75%) patients; the other patient received electrical cardioversion. Figure 4 shows location of the detected rotors and sites with STD and non-continuous fragmentation; globally 44% were related to the pulmonary vein antra, and 72% of patients had rotors or sites with STD related to the pulmonary vein antra.

Ablation and procedural success

Globally, and excluding the patient in whom spontaneous conversion of AF into AT occurred, ablation of rotors or sites with STD was effective in 16/17 patients (*rotor ablation success*: 94.1%); in 6 patients, conversion to sinus rhythm occurred, whereas in the other 10 patients, ablation resulted in stable AT. In 9/17 (53%) patients, the specific rotor or site with STD whose ablation achieved rotor ablation success was located within the pulmonary vein antra. **Supplementary Table 2** shows details about the ATs induced in each patient and the ablation strategy performed; 19 macroreentries and 10 microreentries were found; 5 focal ATs appeared. Considering previous ablations and the index procedure, 11 (61%) patients had PVI, and 15 (83%) patients had CTI ablation.

Procedural success was achieved in 16/18 patients (88.9%). The 2 patients with failed procedure were the one in whom rotor ablation was not effective and electrical cardioversion was needed (empirical PVI plus CTI ablation was performed), and the second was a patient with successful rotor ablation and subsequent ablation of 2 reentrant ATs but with inducibility of another AT that was not ablated afterwards (it was terminated with entrainment maneuvers and no re-inducibility was attempted). There were no procedural complications. In patients with mappable reentrant ATs, the rates of procedural success (92.4%; $p = 0.639$) and procedural complications (11.4%; $p = 0.200$) were similar.

Clinical results

After a mean follow-up of 19.3 ± 15.3 months, and excluding a 3-month blanking period, mean survival free from atrial arrhythmias was 22.1 ± 3.5 months (95% confidence interval [CI]: 15.4–28.9 months). Clinical and procedural variables of patients with and

without recurrences of atrial arrhythmias are shown in Table 2. No statistical comparisons were made due to the limited sample size.

Five patients had arrhythmia recurrences during the blanking period; in 3 of them, electrical cardioversion was performed, with one recurrence after the blanking period; in the other 2 patients, rhythm control strategy was abandoned, and atrioventricular node ablation plus pacemaker implantation was needed. Eight patients had arrhythmia recurrences after the blanking period (including the 2 patients in whom rhythm control was stopped): 5 with AT and 3 with AF; 3 reablation procedures were performed; 2 showed a different reentrant AT, and one showed a gap-related AT. Of the 15 patients with follow-up > 1 year, 10 (66.7%) were free from atrial arrhythmias at a 12-month follow-up.

Mean survival free from atrial arrhythmias in patients with ablation of mappable reentrant ATs during the same period (24.9 ± 2.1 months; 95% CI: 20.7–29.2 months) was similar ($p = 0.740$) (Fig. 5), as well as one-year freedom from atrial arrhythmias (65.8%, $p = 0.946$).

DISCUSSION

We have tested an ablation strategy for unstable reentrant ATs based on focal rotor ablation. To our knowledge, this is the first study that uses driver ablation in patients with reentrant ATs to stabilize unstable circuits.

Ablation of reentrant ATs, excluding CTI-dependent atrial flutter, has shown limited 1-year freedom from atrial arrhythmias in recent reports (51–77%) [1, 5–7]. Moreover, acute procedural success, defined as AT termination into sinus rhythm or conversion to another AT, is not achieved in 10–15% of cases [1, 5–7]. We have obtained, in a cohort of patients classically excluded from other series and considered as especially complex, similar rates of procedural success (88.9%) and 1-year freedom from atrial arrhythmias (66.7%). In patients with mappable reentrant ATs ablated in the same period in our center, results were also comparable. Interestingly, the included patients had less dilated atria than these patients with mappable reentrant ATs; maybe, in a more enlarged atrium, with more dense-scarred tissue and less conduction speed, reentrant circuits are more prone to stabilize.

Rotor identification has to date been based mostly on the use of dedicated catheters and/or software that imply additional costs and time consumption during ablation procedures [14–17]. Conversely, STD analysis as a tool to find rotational activity can be performed with

conventional high-density mapping catheters and is subjectively performed by operators according to visually detectable electrical patterns that show very high (94.3%) interobserver concordance [11]. Of these patterns, the most specific is the finding of a fractionated continuous signal in a single bipole of the mapping catheter, present in almost all regions with dispersion and in almost no regions without dispersion [11]. We hypothesize that fractionated continuous (or quasi-continuous) activity should be visualized within the majority of rotor cores on bipolar signals, as true functional microreentries (Fig. 1A); in fact, fragmentation to consider ‘conventional’ anatomical microreentry has been defined as that comprising > 75% of the tachycardia cycle length [9, 18]. In peripheral regions, however, we believe that spatiotemporal distribution of signals (i.e., all the AF cycle length comprised within the different bipoles of the mapping catheter), which may exhibit some fractionation but not in a continuous manner, could be the most frequent pattern. Besides, finding the rotor pivoting point (i.e., the core) would allow focal ablation, which should be sufficient to stop rotational activity without the need to perform more extensive ablation of all the rotor ‘region’. For these reasons, we decided to use the finding of fractionated quasi-continuous signals on a limited number of adjacent bipoles of the mapping catheter as our definition of rotor. This definition, whether representing or not the true core of rotors, allowed focal ablation with high efficacy in our series.

Another pattern – electrical STD plus non-continuous fragmentation on single bipoles – was used as the marker of rotational activity for patients in whom the former pattern could not be found. We hypothesize that if the rotor core slightly travels with a rotational pattern, fractionated but not continuous activity could be visualized with single bipoles of the mapping catheter located within the travelling trajectory of the rotor core (Fig. 1B). The detection of this pattern is feasible with all the mapping catheters used in this study, but it will show some differences due to the particular architecture of each catheter. When using the IntellaMap ORION catheter, because of its spherical shape, only some splines will be in contact with the tissue and will show EGMs; hence, electrical STD will usually be visualized in some splines. Also, when using PentaRay NAV or Advisor HD Grid (which ideally have the entire mapping surface in contact with the tissue when mapping), electrical STD can usually be found covering the majority of the bipoles (as seen in Fig. 3B).

In patients with AF, conversion rates with driver ablation range between one third [19] and two thirds of cases in most reports [17], with a pooled success rate of 39.6% in a recent meta-analysis [10], although higher efficacies up to 95% have been reported [11]. The high

conversion rate observed in our series could be related to the nature of the arrhythmia; in the continuum between stable reentrant AT and AF, unstable reentrant ATs might exhibit atrial conduction properties less prone to chaotic conduction than AF, and hence easier to stabilize through ablation. Also, the mean number of rotors we found in our cohort (2.0 ± 1.23 rotors per patient) is in the low range of reported data on AF driver ablation (which ranges from 1.8 ± 1.23 to 5 ± 1.5 drivers per patient) [11, 20], although no clear relationship between the number of drivers and ablation success to convert AF seems to exist [10]. The main location of rotors was the pulmonary vein antra (42%), which is a common place for AF drivers. In a study that specifically addressed locations where AF termination was achieved in a cohort of AF patients [16], 27.5% of terminations occurred ablating within the pulmonary vein antra, and in 91% of these locations a rotor was detected.

Another reason that may justify our rotor ablation success rate is a higher short-term spatiotemporal stability of rotors in the context of unstable AT than in AF. Although this affirmation is hypothetical, all rotors that were found through initial mapping in our cohort persisted in the same location when mapping was completed several minutes afterwards. The 10-s criterion to determine temporal stability of rotors in our series was arbitrarily set between reported time criteria, which ranges between 2.5 s and 30 s [11, 21]. However, spatiotemporal stability of drivers in the medium or long term in AF patients has not been demonstrated [22], which might account at least partially (along with atrial disease progression) for arrhythmia recurrences after driver ablation both in AF and unstable AT patients. Indeed, 37.5% of recurrences in our cohort were AF instead of AT.

In this study, we performed PVI only in patients with prior AF diagnosis (11/18 patients). In this subgroup, arrhythmia recurrence rate was numerically lower (4/11 patients, 36%) than in the subgroup of patients without PVI (4/7 patients, 57%), although no statistical comparisons were performed due to the limited sample size. It is possible that routine PVI might decrease atrial arrhythmia recurrence in patients with reentrant AT without previous AF diagnosis, but larger studies are needed to test this hypothesis. Moreover, most patients had rotors or sites with STD within the pulmonary vein antra (72%), and, globally, ablation of a specific rotor or site with STD in this location achieved rotor ablation success in 53% of patients. Hence, we can assume that empirical wide antral PVI (including the ridge between the left atrial appendage and the left superior pulmonary vein, and the posterior interatrial septum) would have had that success rate and would therefore be another valid initial approach for patients with unstable reentrant ATs.

Limitations of the study

The main limitation of this study is the limited sample size, because it was a single-center study and patients with non-mappable reentrant ATs scheduled for ablation are not frequent. Also, because this was an observational study, no comparisons were made with other ablation strategies (e.g., substrate ablation), which may have also been effective; in this regard, we did not perform substrate mapping in sinus rhythm (in patients with initial sinus rhythm) nor use voltage information to guide the initial rotor ablation strategy.

CONCLUSIONS

Most non-mappable reentrant ATs show detectable rotors, identified as sites with single-bipole fractionated quasi-continuous signals, or STD with non-continuous fractionation. Ablation of these sites is highly effective to stabilize the AT or convert it into sinus rhythm.

Conflict of interest: Dr. Eduardo Franco has received consulting fees from Biosense Webster. Dr. Javier Moreno has received consulting fees from Boston Medical, Abbott Medical, and Biosense Webster. The rest of the authors declare no conflicts of interest.

References

1. Anter E, McElderry TH, Contreras-Valdes FM, et al. Evaluation of a novel high-resolution mapping technology for ablation of recurrent scar-related atrial tachycardias. *Heart Rhythm*. 2016; 13(10): 2048–2055, doi: [10.1016/j.hrthm.2016.05.029](https://doi.org/10.1016/j.hrthm.2016.05.029), indexed in Pubmed: [27262767](https://pubmed.ncbi.nlm.nih.gov/27262767/).
2. Patel AM, d'Avila A, Neuzil P, et al. Atrial tachycardia after ablation of persistent atrial fibrillation: identification of the critical isthmus with a combination of multielectrode activation mapping and targeted entrainment mapping. *Circ Arrhythm Electrophysiol*. 2008; 1(1): 14–22, doi: [10.1161/CIRCEP.107.748160](https://doi.org/10.1161/CIRCEP.107.748160), indexed in Pubmed: [19808389](https://pubmed.ncbi.nlm.nih.gov/19808389/).
3. Waldo AL. Pathogenesis of atrial flutter. *J Cardiovasc Electrophysiol*. 1998; 9: S18–S25, indexed in Pubmed: [9727671](https://pubmed.ncbi.nlm.nih.gov/9727671/).

4. Nakagawa H, Shah N, Matsudaira K, et al. Characterization of reentrant circuit in macroreentrant right atrial tachycardia after surgical repair of congenital heart disease: isolated channels between scars allow "focal" ablation. *Circulation*. 2001; 103(5): 699–709, doi: [10.1161/01.cir.103.5.699](https://doi.org/10.1161/01.cir.103.5.699), indexed in Pubmed: [11156882](https://pubmed.ncbi.nlm.nih.gov/11156882/).
5. Coffey JO, d'Avila A, Dukkipati S, et al. Catheter ablation of scar-related atypical atrial flutter. *Europace*. 2013; 15(3): 414–419, doi: [10.1093/europace/eus312](https://doi.org/10.1093/europace/eus312), indexed in Pubmed: [23385050](https://pubmed.ncbi.nlm.nih.gov/23385050/).
6. Ammar S, Luik A, Hessling G, et al. Ablation of perimitral flutter: acute and long-term success of the modified anterior line. *Europace*. 2015; 17(3): 447–452, doi: [10.1093/europace/euu297](https://doi.org/10.1093/europace/euu297), indexed in Pubmed: [25564547](https://pubmed.ncbi.nlm.nih.gov/25564547/).
7. Winkle RA, Moskovitz R, Mead RH, et al. Ablation of atypical atrial flutters using ultra high density-activation sequence mapping. *J Interv Card Electrophysiol*. 2017; 48(2): 177–184, doi: [10.1007/s10840-016-0207-5](https://doi.org/10.1007/s10840-016-0207-5), indexed in Pubmed: [27832399](https://pubmed.ncbi.nlm.nih.gov/27832399/).
8. Takigawa M, Derval N, Frontera A, et al. Revisiting anatomic macroreentrant tachycardia after atrial fibrillation ablation using ultrahigh-resolution mapping: Implications for ablation. *Heart Rhythm*. 2018; 15(3): 326–333, doi: [10.1016/j.hrthm.2017.10.029](https://doi.org/10.1016/j.hrthm.2017.10.029), indexed in Pubmed: [29081399](https://pubmed.ncbi.nlm.nih.gov/29081399/).
9. Strisciuglio T, Vandersickel N, Lorenzo G, et al. Prospective evaluation of entrainment mapping as an adjunct to new-generation high-density activation mapping systems of left atrial tachycardias. *Heart Rhythm*. 2020; 17(2): 211–219, doi: [10.1016/j.hrthm.2019.09.014](https://doi.org/10.1016/j.hrthm.2019.09.014), indexed in Pubmed: [31526822](https://pubmed.ncbi.nlm.nih.gov/31526822/).
10. Baykaner T, Rogers AJ, Meckler GL, et al. Clinical implications of ablation of drivers for atrial fibrillation: a systematic review and meta-analysis. *Circ Arrhythm Electrophysiol*. 2018; 11(5): e006119, doi: [10.1161/CIRCEP.117.006119](https://doi.org/10.1161/CIRCEP.117.006119), indexed in Pubmed: [29743170](https://pubmed.ncbi.nlm.nih.gov/29743170/).
11. Seitz J, Bars C, Théodore G, et al. AF ablation guided by spatiotemporal electrogram dispersion without pulmonary vein isolation: a wholly patient-tailored approach. *J Am Coll Cardiol*. 2017; 69(3): 303–321, doi: [10.1016/j.jacc.2016.10.065](https://doi.org/10.1016/j.jacc.2016.10.065), indexed in Pubmed: [28104073](https://pubmed.ncbi.nlm.nih.gov/28104073/).
12. Waldo AL, Feld GK. Inter-relationships of atrial fibrillation and atrial flutter mechanisms and clinical implications. *J Am Coll Cardiol*. 2008; 51(8): 779–786, doi: [10.1016/j.jacc.2007.08.066](https://doi.org/10.1016/j.jacc.2007.08.066), indexed in Pubmed: [18294560](https://pubmed.ncbi.nlm.nih.gov/18294560/).
13. Saoudi N, Cosio F, Waldo A, et al. Classification of atrial flutter and regular atrial tachycardia according to electrophysiologic mechanism and anatomic bases: a statement from a joint expert group from the Working Group of Arrhythmias of the European Society of Cardiology and the North American Society of Pacing and Electrophysiology. *J Cardiovasc Electrophysiol*. 2001; 12(7): 852–866, doi: [10.1046/j.1540-8167.2001.00852.x](https://doi.org/10.1046/j.1540-8167.2001.00852.x), indexed in Pubmed: [11469446](https://pubmed.ncbi.nlm.nih.gov/11469446/).
14. Narayan SM, Krummen DE, Shivkumar K, et al. Treatment of atrial fibrillation by the ablation of localized sources: CONFIRM (Conventional Ablation for Atrial

- Fibrillation With or Without Focal Impulse and Rotor Modulation) trial. *J Am Coll Cardiol*. 2012; 60(7): 628–636, doi: [10.1016/j.jacc.2012.05.022](https://doi.org/10.1016/j.jacc.2012.05.022), indexed in Pubmed: [22818076](https://pubmed.ncbi.nlm.nih.gov/22818076/).
15. Calvo D, Rubín J, Pérez D, et al. Ablation of rotor domains effectively modulates dynamics of human: long-standing persistent atrial fibrillation. *Circ Arrhythm Electrophysiol*. 2017; 10(12), doi: [10.1161/CIRCEP.117.005740](https://doi.org/10.1161/CIRCEP.117.005740), indexed in Pubmed: [29254947](https://pubmed.ncbi.nlm.nih.gov/29254947/).
 16. Navara R, Leef G, Shenasa F, et al. Independent mapping methods reveal rotational activation near pulmonary veins where atrial fibrillation terminates before pulmonary vein isolation. *J Cardiovasc Electrophysiol*. 2018; 29(5): 687–695, doi: [10.1111/jce.13446](https://doi.org/10.1111/jce.13446), indexed in Pubmed: [29377478](https://pubmed.ncbi.nlm.nih.gov/29377478/).
 17. Quintanilla JG, Alfonso-Almazán JM, Pérez-Castellano N, et al. Instantaneous amplitude and frequency modulations detect the footprint of rotational activity and reveal stable driver regions as targets for persistent atrial fibrillation ablation. *Circ Res*. 2019; 125(6): 609–627, doi: [10.1161/CIRCRESAHA.119.314930](https://doi.org/10.1161/CIRCRESAHA.119.314930), indexed in Pubmed: [31366278](https://pubmed.ncbi.nlm.nih.gov/31366278/).
 18. Lațcu DG, Bun SS, Viera F, et al. Selection of Critical Isthmus in Scar-Related Atrial Tachycardia Using a New Automated Ultrahigh Resolution Mapping System. *Circ Arrhythm Electrophysiol*. 2017; 10(1): e004510, doi: [10.1161/CIRCEP.116.004510](https://doi.org/10.1161/CIRCEP.116.004510), indexed in Pubmed: [28039280](https://pubmed.ncbi.nlm.nih.gov/28039280/).
 19. Atienza F, Almendral J, Ormaetxe JM, et al. RADAR-AF Investigators. Comparison of radiofrequency catheter ablation of drivers and circumferential pulmonary vein isolation in atrial fibrillation: a noninferiority randomized multicenter RADAR-AF trial. *J Am Coll Cardiol*. 2014; 64(23): 2455–2467, doi: [10.1016/j.jacc.2014.09.053](https://doi.org/10.1016/j.jacc.2014.09.053), indexed in Pubmed: [25500229](https://pubmed.ncbi.nlm.nih.gov/25500229/).
 20. Steinberg JS, Shah Y, Bhatt A, et al. Focal impulse and rotor modulation: Acute procedural observations and extended clinical follow-up. *Heart Rhythm*. 2017; 14(2): 192–197, doi: [10.1016/j.hrthm.2016.11.008](https://doi.org/10.1016/j.hrthm.2016.11.008), indexed in Pubmed: [27826130](https://pubmed.ncbi.nlm.nih.gov/27826130/).
 21. Honarbakhsh S, Schilling RJ, Finlay M, et al. Prospective STAR-guided ablation in persistent atrial fibrillation using sequential mapping with multipolar catheters. *Circ Arrhythm Electrophysiol*. 2020; 13(10): e008824, doi: [10.1161/CIRCEP.120.008824](https://doi.org/10.1161/CIRCEP.120.008824), indexed in Pubmed: [32903033](https://pubmed.ncbi.nlm.nih.gov/32903033/).
 22. Jarman JWE, Wong T, Kojodjojo P, et al. Spatiotemporal behavior of high dominant frequency during paroxysmal and persistent atrial fibrillation in the human left atrium. *Circ Arrhythm Electrophysiol*. 2012; 5(4): 650–658, doi: [10.1161/CIRCEP.111.967992](https://doi.org/10.1161/CIRCEP.111.967992), indexed in Pubmed: [22722660](https://pubmed.ncbi.nlm.nih.gov/22722660/).

Table 1. Comparison between clinical variables of the included patients and patients with mappable reentrant atrial tachycardias scheduled for ablation in our center during the inclusion period.

	Included patients (non-mappable ATs) (n = 18)	Other patients (mappable ATs) (n = 79)	P
Age [years]	72.1 ± 8.9	70.5 ± 9.0	0.514
Females	9 (50%)	45 (57%)	0.610
Left ventricular ejection fraction [%]	58 [54–61]	64 [55–71]	0.023
Indexed left atrial volume [mL/m ²]	36.6 ± 11.9	45.8 ± 17.4	0.038
Significant structural cardiopathy	9 (50%)	43 (54%)	0.797
Previous atrial fibrillation	11 (61%)	38 (48%)	0.435
Prior ablation procedures:	11 (61%)	35 (44%)	0.296
Pulmonary vein isolation	5 (28%)	18 (23%)	
CTI ablation	6 (33%)	19 (24%)	
Other reentrant AT ablation	3 (17%)	7 (9%)	
Prior cardiac surgery	4 (22%)	22 (39%)	0.772

Data are shown as mean ± standard deviation, median [interquartile range] or number (percentage), when appropriate; AT — atrial tachycardia; CTI — cavotricuspid isthmus

Table 2. Clinical and procedural variables of patients with and without recurrence of atrial arrhythmias.

	Patients without recurrence (n = 10)	Patients with recurrence (n = 8)
Age [years]	71.1 ± 11.2	73.2 ± 5.3
Females	4 (40%)	5 (63%)
Left ventricular ejection fraction [%]	56 [42–60]	60 [55–66]
Indexed left atrial volume [mL/m ²]	33.6 ± 10.6	40.2 ± 13.0
Significant structural cardiopathy	5 (50%)	4 (50%)
Previous atrial fibrillation	6 (60%)	5 (63%)
Prior ablation procedures	9 (90%)	2 (25%)
Prior cardiac surgery	2 (20%)	2 (25%)
Procedural time [min]	260 ± 66	267 ± 72
Presence of rotors	7 (70%)	6 (75%)
Use of contact force-sensing ablation catheters	3 (30%)	3 (37%)
Pulmonary vein isolation*	7 (70%)	4 (50%)
Cavotricuspid isthmus ablation*	8 (80%)	7 (88%)

*Performed during the index or previous procedures. Data are shown as mean ± standard deviation, median [interquartile range] or number (percentage), when appropriate. No

statistical comparisons between patients with or without recurrence were made because of the limited sample size.

Figure 1. Schematic rationale of rotor detection using a hypothetical 12-pole mapping catheter; **A.** A stable rotor would theoretically show fractionated quasi-continuous electrograms on the bipoles placed on the rotor core (6–7), because the mapping area of that bipole would detect electrical activity during almost all the cycle length. Other bipoles may (or may not) show some degree of fractionation. Red arrow represents rotor spiral wavefront; **B.** If the rotor core meanders around the neighboring tissue, the fractionation would move between different bipoles through time, resulting in non-continuous fractionation. Red arrow represents meandering of the rotor core.

Figure 2. Detailed mapping and ablation approach; *Unstable atrial tachycardia (AT) is defined as having continuous circuit modification; †Spatiotemporal dispersion mapping was biatrial in all patients apart from one, in whom, after failed rotor ablation in the left atrium (LA), sites with spatiotemporal dispersion were successfully targeted in the LA before considering right atrium rotor mapping; AF — atrial fibrillation.

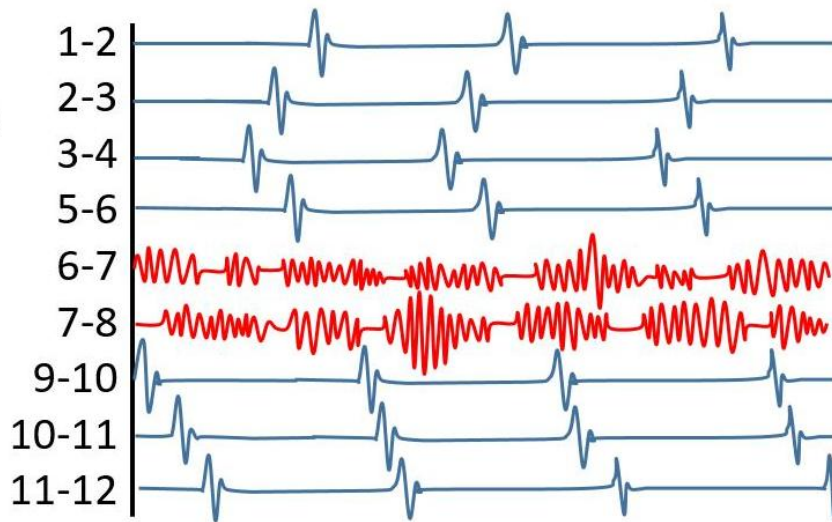
Figure 3. Representative examples of rotors and sites with spatiotemporal dispersion; **A.** Examples of rotors (dotted lines); upper panel and middle panel: IntellaMap ORION catheter; rotors detected in a single bipole; lower panel: Advisor HD Grid catheter; rotor detected in 2 adjacent bipoles (D1–D2 and D2–D3); note the low voltage of electrical signals in the middle and lower panel; **B.** Examples of sites with spatiotemporal dispersion and non-continuous fractionation (dotted lines); arrows represent hypothetical trajectory of a meandering rotor core; upper panel: IntellaMap ORION catheter; middle panel: PentaRay NAV catheter (PR); lower panel: Advisor HD Grid catheter; paper speed: 200 mm/s; ORB — Woven Orbiter catheter; blue bipoles around tricuspid annulus and green bipoles into the coronary sinus.

Figure 4. Location of rotors (pink dots) and sites with spatiotemporal dispersion and non-continuous fragmented electrograms (green dots). Eleven (42%) rotors were related to the antra of the pulmonary veins, especially the anterior aspect of the right superior pulmonary vein (n = 6) and the ridge between the left atrial appendage and the left superior pulmonary vein (n = 4); CS — coronary sinus; FO — foramen ovale; IVC — inferior vena cava; LIPV — left inferior pulmonary vein; LSPV — left superior pulmonary vein; RIPV — right

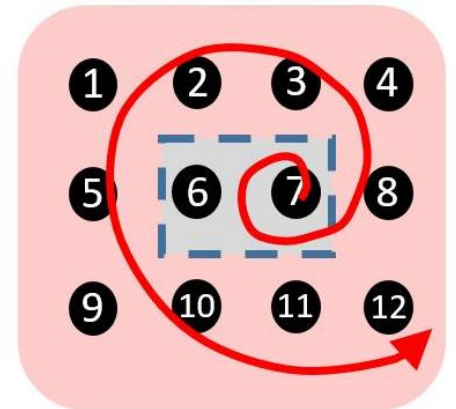
inferior pulmonary vein; RSPV — right superior pulmonary vein; SVC — superior vena cava.

Figure 5. Estimated survival free from atrial arrhythmias, excluding a 3-month blanking period, in included patients and patients with ablation of mappable reentrant atrial tachycardias (ATs) during the same period.

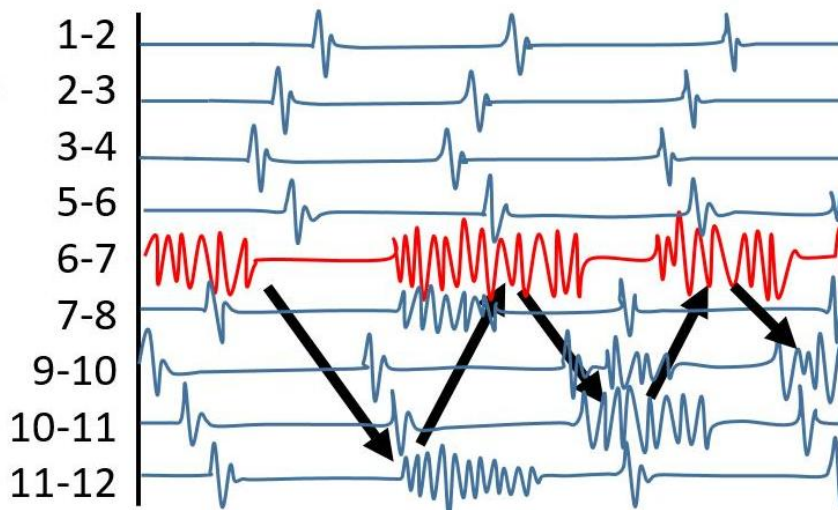
A



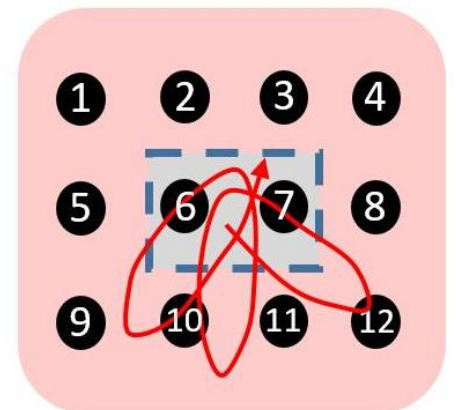
ROTOR WAVEFRONT

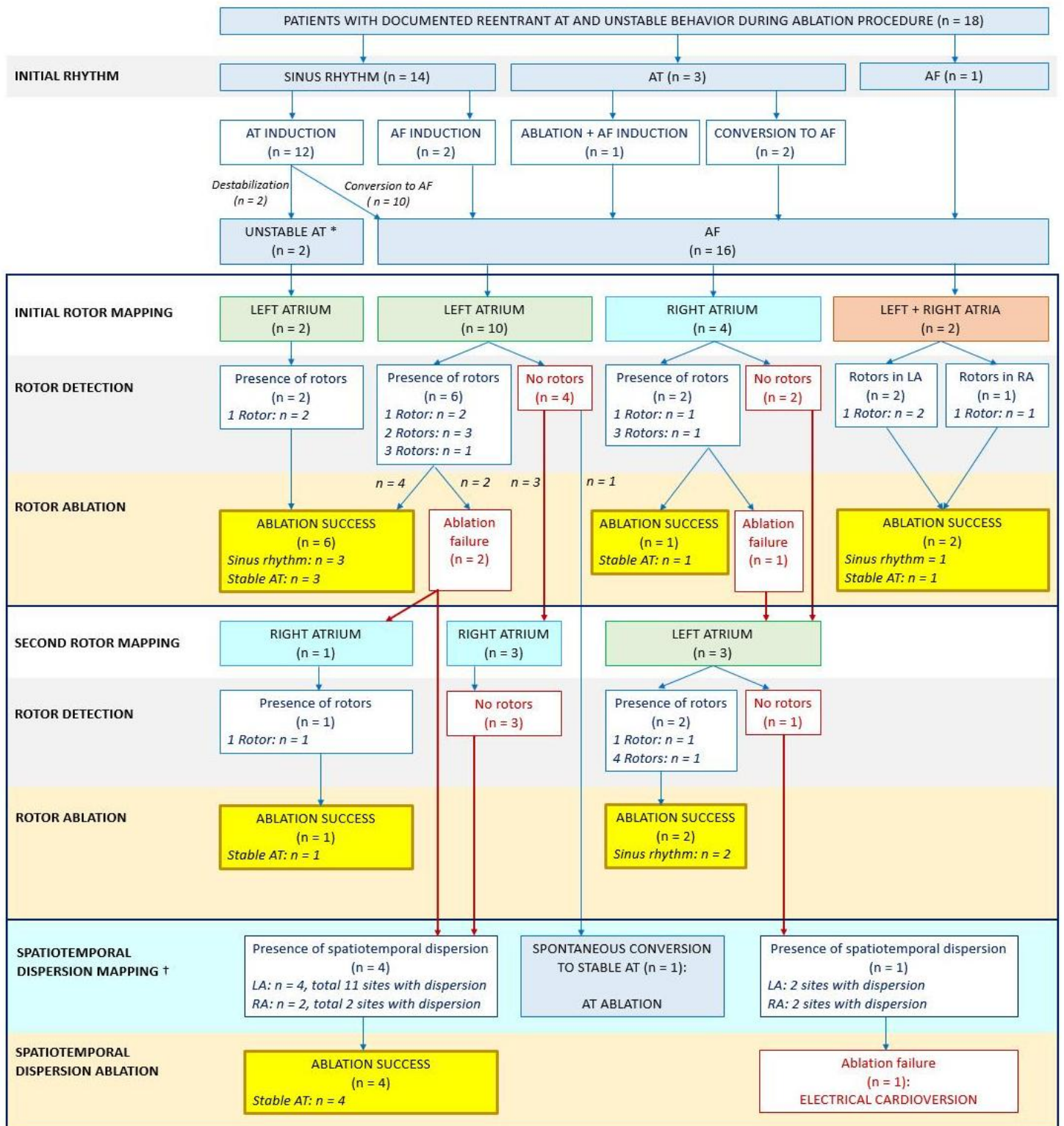


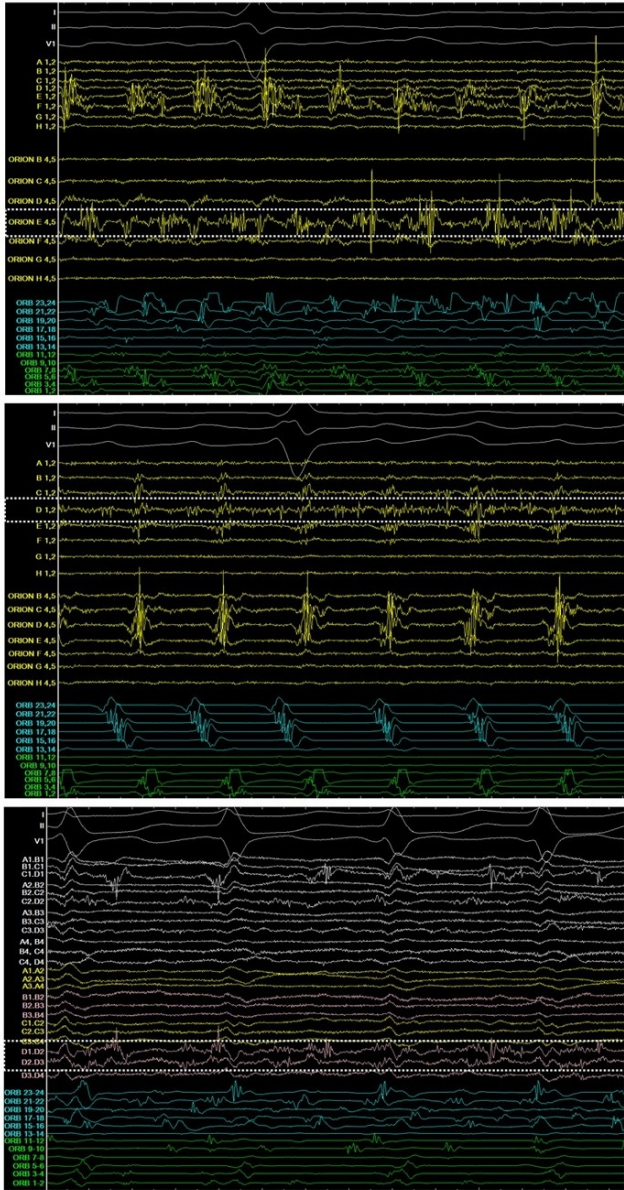
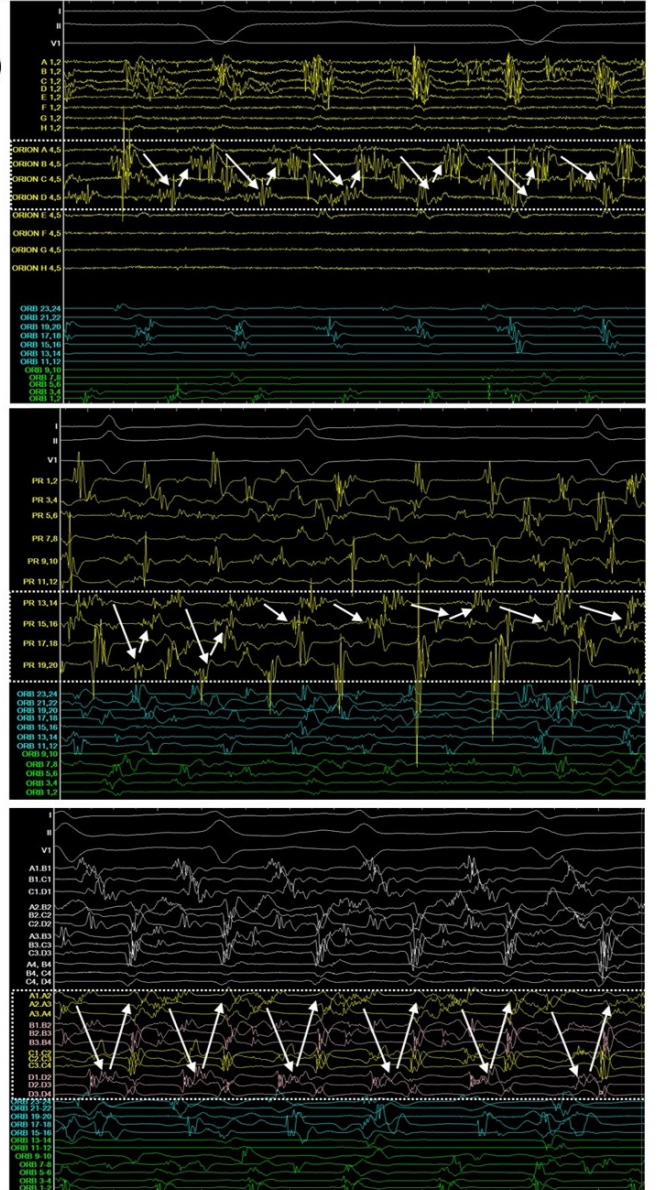
B



CORE MEANDERING

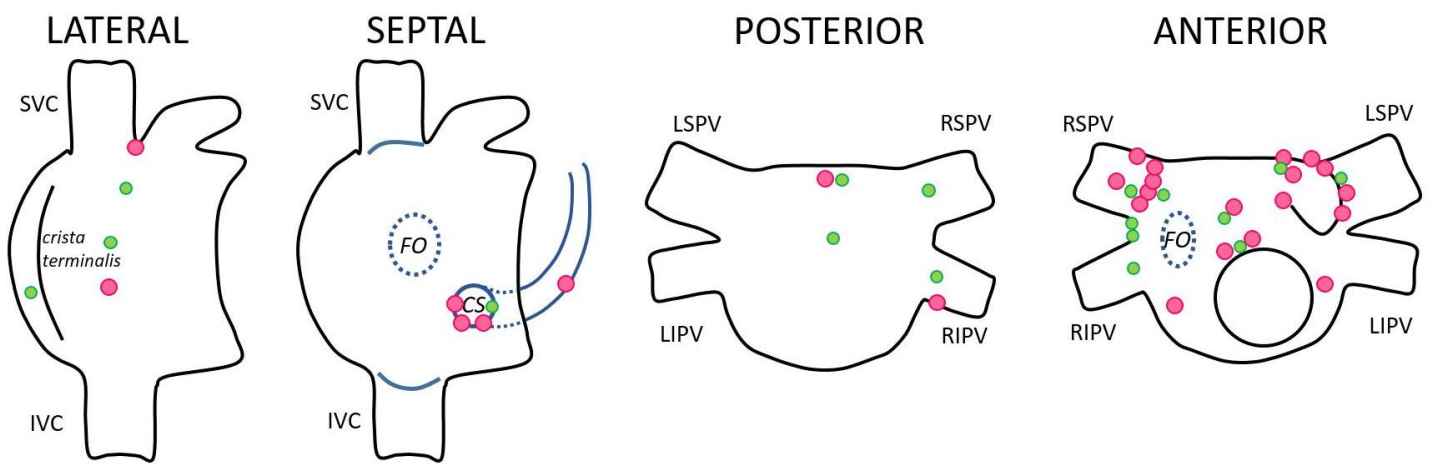




A**B**

ROTORS IN THE RA, n = 6.

ROTORS IN THE LA, n = 20.



Sites with spatiotemporal dispersion and non-continuous fractionation, n = 17.

